



# Combustion Characteristics and Emissions of Biodiesel/Natural Gas Dual Fuel Engine

S. M. J. Yahyaei, A. Gharehghani<sup>†</sup>, and M. Targolghasemi

*School of Mechanical Engineering, Iran University of Science and Technology, Tehran, Iran*

<sup>†</sup>Corresponding Author Email: [ayat\\_gharehghani@iust.ac.ir](mailto:ayat_gharehghani@iust.ac.ir)

## ABSTRACT

Strict emission regulations together with reducing fossil fuels resources lead to more attention on new combustion strategies and alternative fuels such as biodiesel which is renewable, environmentally friendly and more cost-effective than other fuels. In this study, CONVERGE CFD software coupling with chemical kinetics mechanism is used to numerically investigation of natural gas (NG)/biodiesel dual fuel engine. The discussed biodiesel consists of 25% methyl decanoate (MD), 25% methyl-9-decanoate (MD9D) and 50% diesel. A comparative study of NG/diesel and NG/biodiesel fueled cases is performed to highlight the combustion characteristics of biodiesel. For all simulated cases, it is supposed that 5% of energy is supplied by high reactive fuel (i.e., Diesel or Biodiesel) and 95% is coming with low reactive fuel (i.e., Natural Gas). Results revealed that in full load condition, using biodiesel/NG led to 86% lower carbon monoxide (CO) and 91% unburned hydrocarbons (UHC). On the other hand, peak pressure and maximum in-cylinder temperature increased 5% and 83 K, respectively which led to 0.6% efficiency improvement. according to the results of different injection timing, when it was advanced from -4 to -20 crank angle degree after top dead center (CAD ATDC) for biodiesel/NG and diesel/NG, the indicated mean effective pressure (IMEP) and gross thermal efficiency (GTE) reached at their peaks 18.3 bar and 48.2% at -12 CAD ATDC, 18.05 bar and 47.7% at -8 CAD ATDC respectively.

## Article History

*Received January 5, 2024*

*Revised February 17, 2024*

*Accepted March 8, 2024*

*Available online May 29, 2024*

## Keywords:

*Dual fuel*

*NG/Biodiesel*

*NG/Diesel*

*Numerical simulation*

*Injection timing*

## 1. INTRODUCTION

Due to the increasing demand for energy as well as the projected shortages of petroleum fuels and their rising prices, fossil fuels are highly concerned. The increase in consumption contributes significantly to global warming and climate change (Sanjeevannavar et al., 2022). As a result of the strict laws established to protect the environment, researches have devoted most of their efforts to reducing the amount of pollution emissions in different ways (Reitz & Duraisamy, 2015a). Researchers have proposed various solutions to deal with this challenge and to lower the pollutants emitted, such as using different fuels, applying after-treatment systems, and adopting new combustion strategies (Reitz & Duraisamy, 2015b; Wei & Geng, 2016; Duan et al., 2021; Paykani et al., 2021; Bhave et al., 2022; Paykani et al., 2022; Hosseini et al., 2023). Natural gas is a composite of various gases, including methane, ethane, and others. Methane constitutes the majority of natural gas, accounting for 87-96% of its composition. Consequently, natural gas shares many

properties akin to methane. It is widely acknowledged as a clean and eco-friendly fuel, owing to its lower carbon content per unit of energy compared to other fossil fuels, resulting in reduced CO<sub>2</sub> emissions (Huang et al., 2019; Mikulski et al., 2019; Poorghasemi et al., 2017; Yuvenda et al., 2022). Dual fuel engines represent a combustion technique that employs two distinct fuels possessing dissimilar physical and chemical characteristics. These fuels are utilized as high-reactivity and low-reactivity fuels, respectively. The dual fuel mode has the benefit that the diesel start of injection can regulate the combustion phasing. Diesel injection timing in a dual fuel engine resulted in a reduction in emissions and unburned methane at low loads (Yousefi et al., 2019a; 2020; Pedrozo et al., 2022; Fakhari et al., 2024). Natural gas is utilized as a low-reactivity fuel in dual fuel engines due to its low carbon to hydrogen ratio. This is particularly advantageous as it results in a reduction of CO<sub>2</sub> emissions by over 20% when compared to diesel engines. In dual fuel engines, natural gas is introduced into the combustion chamber in a homogenous manner through the use of port injection and

Nomenclature			
AMR	Adaptive Mesh Refinement	IVC	Intake Valve Closing
ATDC	After Top Dead Center	KH-RT	Kelvin-Helmholtz Rayleigh-Taylor
BTE	brake Thermal Efficiency	LTC	Low Temperature Combustion
CAD	Crank Angle Degree	MD	Methyl Decanoate
CDF	Conventional Dual Fuel	MD9D	Methyl-9-Decenoate
CFD	Computational Fluid Mechanic	NG	Natural Gas
CNG	Compressed Natural Gas	NO <sub>x</sub>	Nitrogen Oxide
CO	Carbon Monoxide	NTC	Non-Timed Collision
EVO	Exhaust Valve Opening	PCCI	Premixed Charged Compression Ignition
GTE	Gross Thermal Efficiency	RCCI	Reactivity Controlled Compression Ignition
HRR	Heat Release Rate	RPM	Revolution Per Minute
HCCI	Homogeneous Charged Compression Ignition	SOI	Start of Injection
ID	Ignition Delay	UHC	Unburned Hydro Carbon
IMEP	Indicated Mean Effective Pressure	ITE	Indicated Thermal Efficiency

is subsequently mixed with air. In contrast, diesel fuel is directly injected into the chamber. Furthermore, dual fuel engines exhibit reduced levels of soot and NO<sub>x</sub> emissions when compared to conventional diesel engines. Additionally, these engines possess the ability to maintain and enhance the benefits of diesel engines, while also exhibiting superior performance in medium and high load conditions. Numerous studies have been conducted in diverse fields pertaining to dual-fuel engines utilizing the combination of natural gas and diesel fuel (Korkmaz et al., 2019; Wu et al., 2019; Gharehghani et al., 2021; Park et al., 2022; Yu et al., 2022; Park et al., 2023; Wei et al., 2023; Yin et al., 2023). Liu et al. (2023) conducted an investigation into the augmentation of energy ratio in a dual fuel engine utilizing natural gas and diesel fuel at a 25% load. The results indicated that as the energy ratio of natural gas increased, the maximum pressure exhibited a pattern of decreasing followed by increasing, and the heat release rate (HRR) curve transitioned from a one-stage to a two-stage state. Furthermore, the ignition delay was observed to decrease, while the quantity of NO<sub>x</sub> pollutants followed a trend of initial increase followed by subsequent decrease. (Shu et al., 2018) conducted an investigation on the impact of advanced injection timing in a diesel/natural gas twin burner engine. The study involved an initial assessment of the brake thermal efficiency (BTE) value, followed by a gradual reduction as the degree of pilot injection increased. The observed increase in NO<sub>x</sub> content was attributed to the rise in the mass fraction of oxygen atoms and the temperature within the combustion chamber. Lee et al. (2020) studied optimization of diesel injector in the heavy-duty dual fuel engine. With a reduction in hole diameter of nozzle, gross IMEP increases and this increase is about 1.66% in the optimal mode. (Yousefi et al., 2019b) investigated natural gas/diesel combustion at low load by highlighting greenhouse gas emissions. Due to greater accessibility and lower environmental effects, substituting diesel with natural gas is more common in industries. Also, the effect of additives on dual-fuel engines has also been investigated (Dal Forno Chuahy et al., 2021; Mattarelli et al., 2022; Fakhari et al., 2023; Thangavel et al., 2023). As mentioned, diesel fuel is used as high reactive fuel in dual fueling mode as igniter of combustion. Biodiesel is the ideal alternative for diesel fuel, not only because of its similarity to diesel, but also because of its higher cetane

number and also containing oxygen atom in its chemical structure. Therefore, biodiesel is suitable high reactive fuel which could lead to lower amounts of CO and HC emissions (Kalsi & Subramanian, 2017; Mahla et al., 2018; Wenming & Meng, 2019; Thomas et al., 2020; Karami & Gharehghani, 2021; Zarrinkolah & Hosseini, 2022; Winangun et al., 2023). Harari et al. (2020) conducted a study on the emission characteristics associated with the use of gasoline and biodiesel derived from *Thevetia Peruviana*. They showed that HC and CO emissions decreased by 12.5% and 7.6% respectively by using biodiesel as high reactive fuel. The presence of oxygen and high cetane number of biodiesel lead to stable and faster combustion, which resulted in more complete combustion (Gharehghani et al., 2015; Işik & Aydin, 2019; Jain et al., 2023; Rajpoot et al., 2023; Vargas-Ibáñez et al., 2023). Zhang et al. (2022) Analyzed various biodiesel to natural gas ratios in a dual-fuel marine engine. When natural gas energy and biodiesel to diesel ratio increased, combustion begins later and thermal efficiency declines. NO<sub>x</sub> emission was reduced by using more natural gas energy and burning it longer, which lowered the temperature and pressure inside the cylinder. Due to high surface tension and greater viscosity of biodiesel, combustion delay increased by increasing the biodiesel ratio. Cheng et al., (2015) They studied the chemical synthesis mechanism in detail using reduction techniques and temperature sensitivity analysis for a variety of biodiesel fuels. The simulation results, in turn, demonstrate that the vital species and reactions to combustion processes are preserved in the reduced biodiesel mechanism of 92 species. The IDs and lift-off lengths are accurately reproduced by the reduced mechanism, with maximum percentage errors of 29.8% and 43.4%, respectively. Mohan et al. (2015) A new skeletal multicomponent fuel reaction mechanism is proposed, which consists of MD, MD9D, n-heptane and iso-octane. The final mechanism consisted of 68 species and 183 reactions. Kumar et al. (2022) investigated adding hydrogen to biodiesel in a dual-fuel engine. By adding hydrogen to biodiesel and increasing injection pressure, pressure and temperature inside the chamber and brake thermal efficiency (BTE) increased. They showed that by increasing the injection pressure, the fuel atomization improved, and as a result, the ignition delay decreased. Rajpoot et al. (2023) investigates spirulina microalgae

biodiesel with energy exergy emission evaluations of a diesel engine. There are multiple fuel samples. Only one third of the input energy is available for useful work while two third is related with energy losses. The pollutants emission was reduced by up to 28.09%. this study shows that microalgae biodiesel can be a good replacement for conventional fuels. Biodiesel has advantages over diesel in terms of combustion quality, renewability and environmental impact. In addition, natural gas is a low-cost and clean fuel with a low carbon-to-hydrogen ratio. As far as the authors are aware, no study has thoroughly compared the dual fuel combustion mode of diesel/natural gas and biodiesel/natural gas fuels. Therefore, this study investigates numerical simulation of biodiesel/natural gas and its comparison with diesel/natural gas in a 6-cylinder dual fuel engine in terms of combustion quality and pollutants. The study also examines how the injection timing of biodiesel affects the combustion process and engine-out emissions of biodiesel/NG. For all simulated cases, it is supposed that 5% of energy is supplied by high reactive fuel (i.e., Diesel or Biodiesel) and 95% is coming with low reactive fuel (i.e., Natural Gas).

## 2. NUMERICAL MODELING

The numerical simulations conducted in this study utilized the CONVERGE software to accurately represent the combustion processes and formation of pollutants. To model the atomization of fuel droplets, a combination of the Kelvin Helmholtz and Riley Taylor models was employed, while droplet collisions were simulated using the non-timed collision model. Additionally, the simulation incorporated models for heat transfer effects and turbulence.

### 2.1 Computational Model, Tools, Methods and Mechanism

Computational domain is the geometry of a six-cylinder turbocharged diesel engine with a common rail injection system. Engine specifications are listed in (Table 1).

In this research, the engine is considered at 1000 rpm and at 100% load. (Table 2) shows diesel, biodiesel and natural gas properties.

As mentioned, this research utilized Converge software for numerical simulations. The combustion processes and pollutant formation were modeled using a

**Table 1 Engine parameters and specifications (Shu et al., 2019)**

Item	Content
Displacement (L)	9.726
Bore (mm)	126
Stroke (mm)	130
Compression ratio	17
Connecting rod length (mm)	219
Injector spray angle (°)	147
Number of injector nozzle holes	8
IVC (°CA)	-155
EVO (°CA)	120

**Table 2 Properties of diesel, biodiesel and natural gas**

	Diesel	Biodiesel	NG
Low heat value (MJ/Kg)	44.6	41	50
Cetane index	50	51.5	-
Density (Kg/m <sup>3</sup> )	830	870-880	-
Kinematic viscosity (N.s/m <sup>2</sup> )	3.4	4.142	-
surface tension (N/m)	0.015-0.014	0.020-0.019	-
specific heat (J/Kg. K)	2458.82	2375.82	-
Conductivity (W/m. K)	0.11	0.12- 0.14	-

set of sub-models. The fuel droplets' atomization was modeled by combining the Kelvin Helmholtz model and the Riley Taylor model (KH-RT). The KH-RT hybrid atomization model consists of two primary and secondary breakups. Kelvin-Helmholtz (KH) wave models were employed to predict the primary breakup of the jet, and Rayleigh-Taylor (RT) breakup models were used to model the secondary breakup of drops after a breakup length along with KH (Beale & Reitz, 1999). The droplet collisions and their effect on spray modeling were modeled using the non-timed collision (NTC) model. The NTC method randomly picks some packets in each cell to speed up the collision calculations (Schmidt & Rutland, 2000). Heat transfer influenced the combustion quality and the thermodynamic properties, and so did the walls' heat transfer effects. Various factors that affect this phenomenon, like flow turbulence, wall heat transfer and gas density change, were modeled. The heat transfer between the wall and the turbulent flow was modeled by taking into account the density and Prandtl number at each step of the solution (Schmidt & Rutland, 2000). The modeling of NO<sub>x</sub> formation has been done using the developed ZELDOVICH mechanism provided. RANS mechanism was used for turbulence modeling. Also, the (RNG) k-ε model is used as a turbulence model with modified rapid distortion and the wall function model of Hahn and Reitz. The engine combustion process is modeled using the SAGE model, which is an accurate chemical kinetic model. The simulations were performed using the multi-zone chemistry solver, and in the multi-zone chemistry solver, based on the thermodynamic state of the cells, cells are grouped into regions, and detailed chemical kinetics are solved in each region to reduce execution time. In the chemical mechanism, n-heptane has been chosen as a representative of diesel and methane as a representative of NG. Also, it is supposed that biodiesel consists of 25% MD, 25% MD9D and 50% n-C7H16. The authors have previously published the details of this mechanism, which consists of 126 species and 545 chemical reactions.

### 2.2 Computational Domain and Validation

The dynamic mesh is created using the geometry of a six cylinders diesel engine. A piston model with one-eighth of the size and an injector spray angle of 147° is used due to the symmetry of the eight holes in the nozzle.

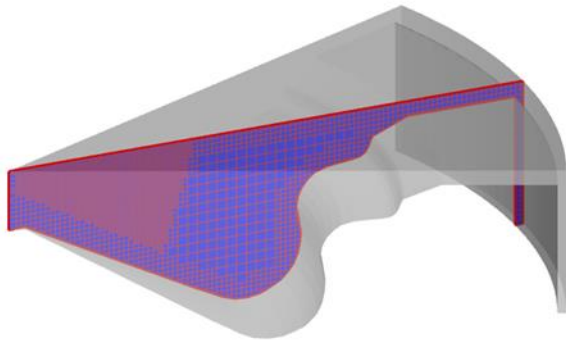


**Fig. 1** CFD model of combustion chamber with one eighth of the size

**Table 3** The initial and boundary conditions of validation case

Items	Values
Engine speed	1000 RPM
Start of Injection (SOI)	-5 CAD ATDC
Injection Duration (ID)	3 CAD
Intake pressure	2.006 bar
Lambda	1.301
CH4 mass fraction	0.0389
Cylinder Head Temperature	523 K
Cylinder Block Temperature	433 K
Piston Temperature	553 K

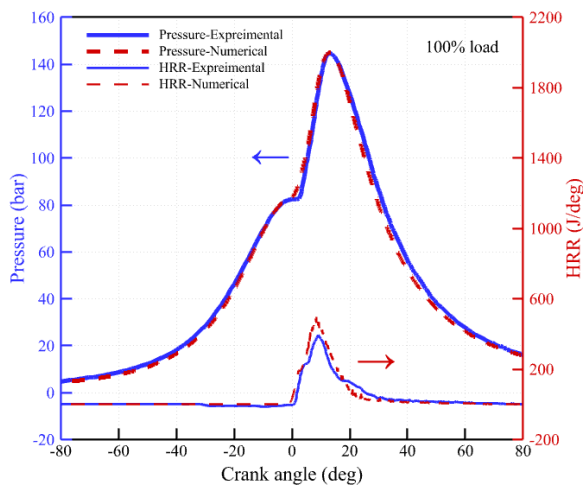


**Fig. 2** Comparisons of experimental and simulated in-cylinder pressure and HRR results at 100% load

Figure 1 shows the geometry of one eighth piston. The grid size is 1.2 mm and the adaptive mesh refinement (AMR) method and fixed embedding are used for spray and inflation near boundaries to get a fine enough grid. AMR is applied for temperature and velocity field in the volume with diesel (biodiesel) and injected particles. The calculation covers from intake valve closing (IVC= -155 CAD) to exhaust valve opening (EVO= +120 CAD). (Table 3) lists the initial and boundary conditions for simulations.

The in-cylinder pressure and heat release rate are shown in (Fig. 2) to compare the numerical and

**Table 4** Experimental and simulated emission results at 100% load

Emissions (ppm)		NOx	HC	CO
	Experimental (Shu et al., 2019)	3144	682	65
	Numerical	2980	722	58

experimental results. The simulated and experimental pressure agree well and have a negligible difference. The maximum difference between this numerical study and experimental data is less than one percent. The heat release rate in the simulation also matches the experimental data closely.

In addition, the simulated and experimental NOx, HC and CO emissions are compared in (Table 4). The error is less than 8% at most. Therefore, the CFD model can accurately simulate the combustion and ignition processes.

### 3. RESULTS AND DISCUSSION

#### 3.1 Comparing Biodiesel/NG and Diesel/NG Combustions

This study compares the combustion characteristics of diesel/NG and biodiesel/NG in dual fuel mode. Figure 3 shows the in-cylinder pressure and heat release rate at 1000 rpm and full load condition. The diesel/NG case has a peak pressure of 144.3 bar at 13.1 CAD ATDC, while the biodiesel/NG case has a peak pressure of 151.7 bar at 14.5 CAD ATDC. Biodiesel is more reactive than diesel because it has a higher cetane number and oxygen content. This makes the biodiesel/NG mixture more reactive than the diesel/NG mixture. The higher reactivity gradient causes the higher peak pressure of biodiesel/NG case.

Figure 4(a) compares in-cylinder mean temperature for diesel/NG and biodiesel/NG fueling cases. As seen, biodiesel/NG case has about 3.8% higher maximum

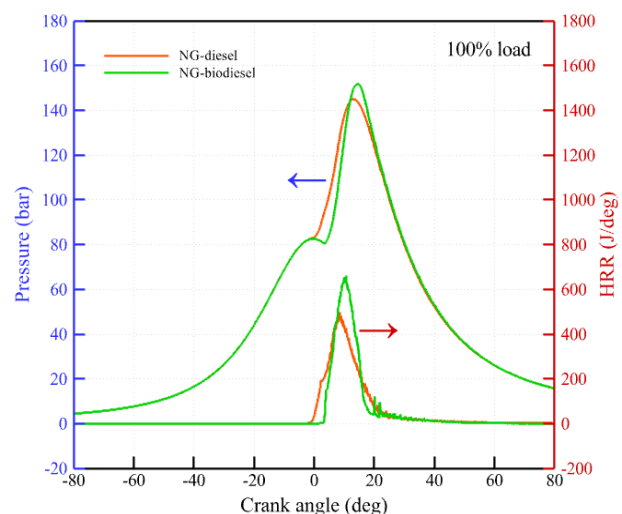


**Fig. 3** In-cylinder pressure and heat release rate for biodiesel/NG and diesel/NG at 100% load

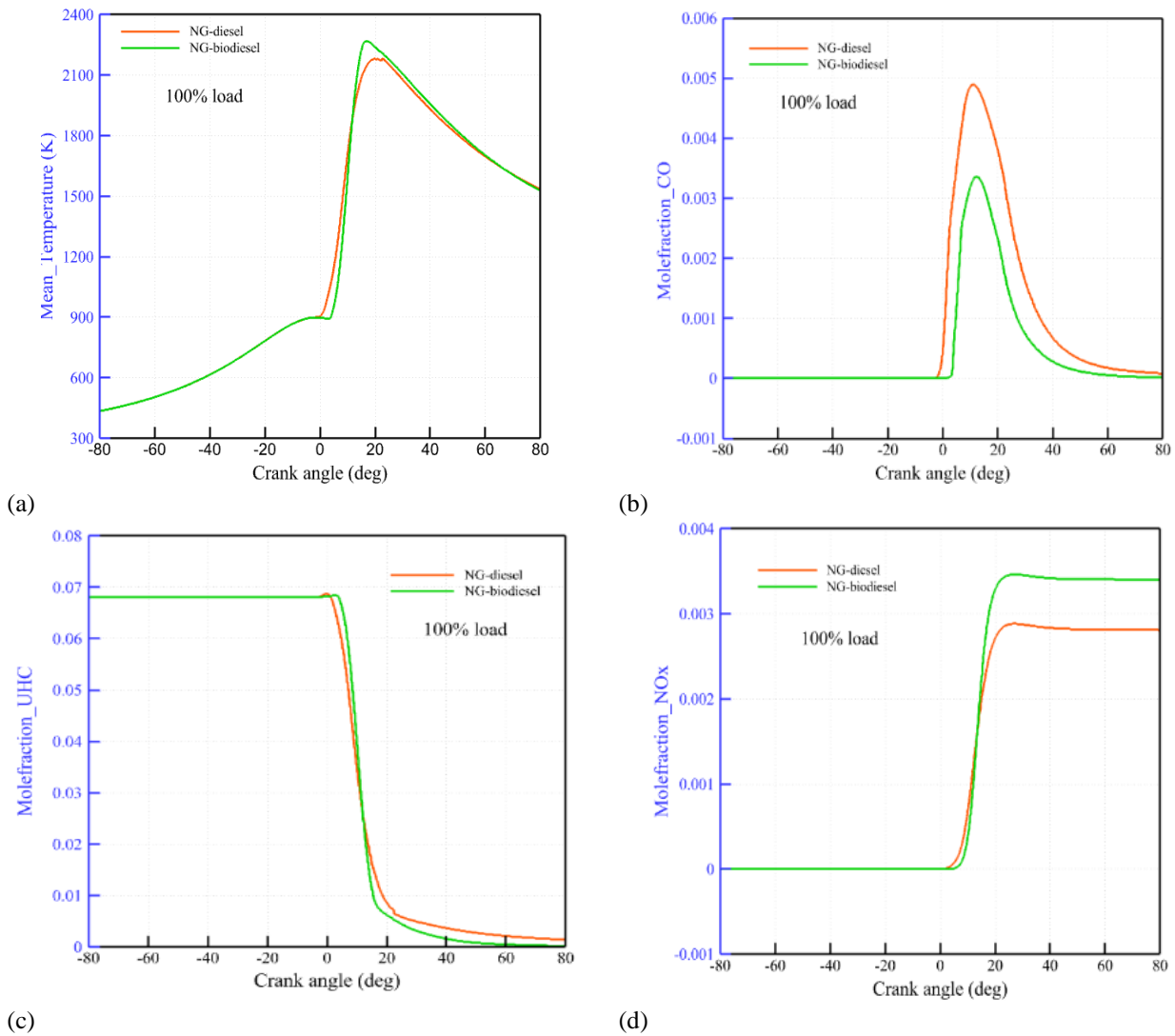


**Fig. 4 Comparison of NG/diesel and NG/biodiesel combustion in terms of a) mean in-cylinder temperature b) mole fraction of NOx c) mole fraction of UHC and d) mole fraction of CO**

temperature than diesel/NG. Also, the maximum in-cylinder temperature in biodiesel/NG case occurs at 16.9 CAD ATDC, while in diesel/NG its location is at 22.5 CAD ATDC. One of the advantages of biodiesel is that the combustion timing is shorter than that of diesel. In the biodiesel/NG case, the combustion timing is approximately 15.2 degrees, while it is approximately 19.6 degrees in a diesel/NG case. Biodiesel/NG burns 4.5 degrees faster than diesel/NG, while diesel/NG CA50 occurs faster than biodiesel/NG. CA50 amount for diesel/NG case is 10.4 ATDC while in biodiesel/NG it is about 11.0 ATDC. As mentioned, the cetane number of biodiesel is higher than that of diesel, resulting in an increase in reactivity of mixture. In addition, due to the higher surface tension of biodiesel, ignition delay of biodiesel/NG increases and leads to the better mixing and results into the improving combustion quality and higher in-cylinder pressure and temperature.

Better combustion quality of biodiesel/NG fueling case affects the engine-out emissions. There is a significant reduction in carbon monoxide (CO) in biodiesel/NG case compared to diesel/NG. As shown in (Fig. 4 b), CO engine-out emission decreases 86% for

biodiesel/NG compared to diesel/NG. This is because biodiesel has higher oxygen content and lower carbon-to-hydrogen ratio than diesel, which enhances the oxidation of fuel and reduces the formation of CO. Also, UHC emission is lower in biodiesel/NG fueling case (Fig. 4 c). This is because biodiesel has lower volatility and higher cetane number than diesel, which improves the vaporization and ignition of fuel and reduces the UHC emission. On the other hand, NOx emission level is about 24% higher for biodiesel/NG fueling case. More complete combustion of biodiesel/NG case and as result higher in-cylinder temperature leads to higher amount of NOx emission (Fig. 4 d). This is because biodiesel has higher nitrogen content and higher flame temperature than diesel, which increases the production of NOx through thermal and prompt mechanisms. Therefore, biodiesel/NG case has lower CO and UHC but higher NOx emissions than diesel/NG case.

Figure 5 shows the contours of NOx and CO emissions in exhaust valve opening (EVO) crank angle location. Higher ignition delay of biodiesel causes better mixing for biodiesel/NG case and as result, complete combustion leads to lower CO emission while NOx emission level

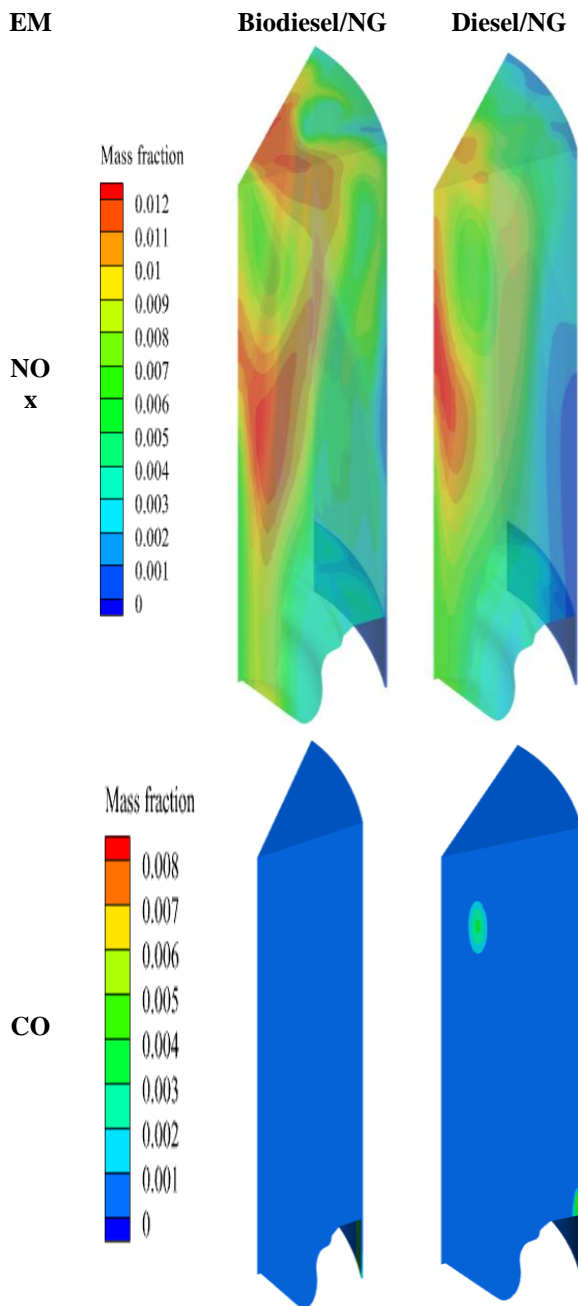


**Fig. 5** NO<sub>x</sub> and CO contour at EVO

increases for this case. This is because biodiesel has higher oxygen content and lower carbon-to-hydrogen ratio than diesel, which enhances the oxidation of fuel and reduces the formation of CO. However, biodiesel also has higher nitrogen content and higher flame temperature than diesel, which increases the production of NO<sub>x</sub> through thermal and prompt mechanisms. Therefore, biodiesel/NG case has lower CO but higher NO<sub>x</sub> emissions than diesel/NG case.

Table 5 shows the CA10, CA50 and CA 90 for biodiesel/NG and diesel/NG. As shown, diesel/NG case has lower CA10 than biodiesel/NG, while combustion duration of biodiesel/NG has lower combustion duration (CA90-CA10). This is because biodiesel has higher cetane number and lower volatility than diesel, which causes a longer ignition delay and a later start of combustion.

**Table 5** CA10, CA50 and CA90 for Biodiesel/NG and Diesel/NG

	CA10	CA50	CA90
Diesel/NG	4.13	10.41	23.77
Biodiesel/NG	6.51	11.01	21.7

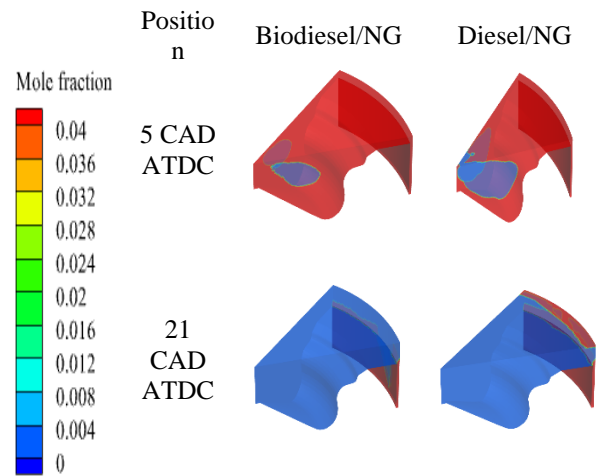


**Fig. 6** Methane mole fraction distribution at 5 and 21 CAD ATDC for diesel/NG and biodiesel/NG

However, higher ignition delay improves the mixing quality. More homogeneous mixture together with higher oxygen content of biodiesel leads to faster combustion rate and a shorter combustion duration in biodiesel/NG case.

Figure 6 shows the methane mole fraction in 5 and 21 CAD ATDC. It can be seen that in 5 CAD ATDC, biodiesel/NG case has more unburned methane than diesel/NG case. However, in 21 CAD ATDC, biodiesel/NG case has less unburned methane than diesel/NG case.

Mass fraction of OH species and temperature distribution of parcels for diesel and biodiesel are shown in (Fig. 7). As seen, during the combustion of diesel, ignition takes place in the center of the parcels and then propagates upstream and downstream. While for biodiesel, parcels are distributed more homogeneously before start of combustion and ignition occurs under the auto ignition dominance, with flame front propagation focusing toward the perimeter of the cylinder. As shown, CA1 (crank angle where 1% of heat is released), diesel injection length is 16 mm while for biodiesel injection length is 25 mm. Due to biodiesel's high surface tension and greater viscosity, evaporation is delayed and as result, penetration length increased which leads to later start of combustion. On the other hand, based on Fig. 7, biodiesel parcels have higher temperature than diesel parcels before SOC, and as result, combustion duration of biodiesel/NG is shorter than diesel/NG case see (Table 5).

In (Fig. 8), the volume with temperature lower than 2000 K is shown for biodiesel/NG and diesel/NG cases at 7 CAD ATDC. The volume with temperature lower than 2000 K is the main source of incomplete combustion and leads to formation of CO pollutant. Higher temperature of biodiesel/NG combustion together with better mixing

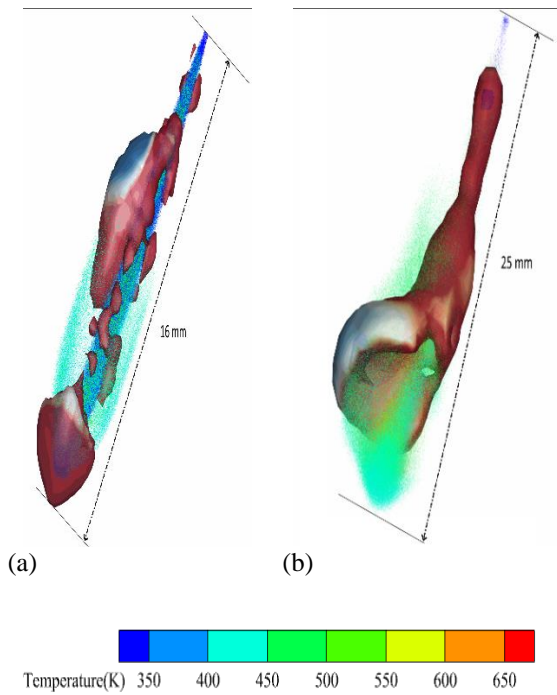
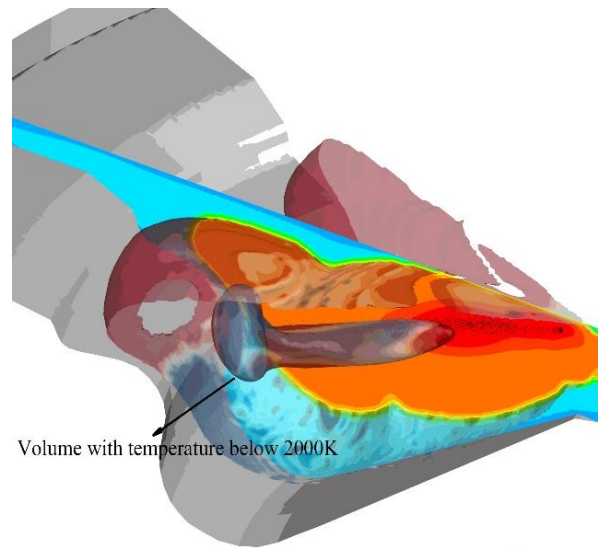


**Fig. 7 The OH mass fraction in bulk in CA1 and parcels temperatures a) diesel b) biodiesel**

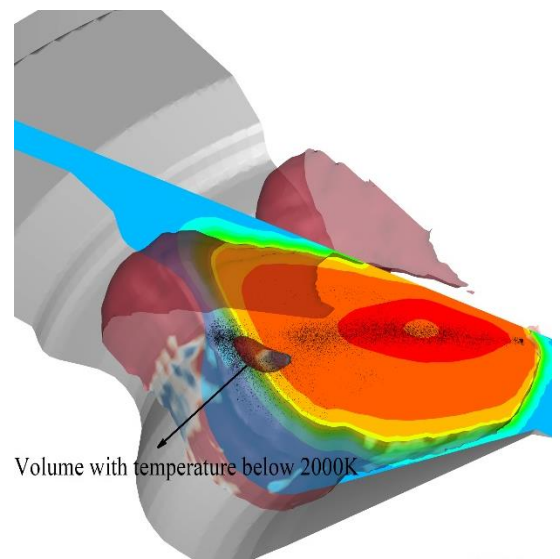
condition, causes minor lump region for this case and as result, lower CO emission compared to diesel/NG case based on (Fig. 5).

### 3.2 Effect of Start of Injection on Combustion Characteristics

This section examines the effect of advancing the injection timing (SOI) on the engine performance characteristics of biodiesel/NG and diesel/NG dual fuel mode. The study tested a range of SOI from  $-4$  to  $-20$  CAD ATDC at full load condition. Figure 9 shows the results of the study for in-cylinder pressure, HHR and (Fig. 10) in-cylinder mean temperature. According to Fig. 9 by advancing the injection timing from  $-4$  to  $-20$  CAD ATDC, in biodiesel/NG the peak pressure value rises from 150.2 to 205 bar but in diesel/NG the peak pressure value rises from 143.1 to 202.6 bar. Moreover, as seen, in Fig. 10 the trend of in-cylinder temperature follows the change in injection timing, indicating that the change in combustion characteristics also follows the change in injection timing. By advancing the SOI, ignition delay increased and mixing quality is enhanced. Long ignition delay together with good mixing situation provide more favorable condition for start of combustion. As a result, combustion quality improves and causes higher in-cylinder pressure and temperature. By advancing the injection timing from  $-4$  CAD ATDC to  $-20$  CAD ATDC, heat is released earlier during the combustion process and the peak of heat release rate is consistently increased. This increase in biodiesel/NG is more than diesel/NG. This is mainly because biodiesel fuel has enough time to be available, evaporate, and spread in the combustion chamber, which enhances the oxidation of methane fuel. The combustion of biodiesel fuel gives the activation energy needed for the combustion of methane to happen sooner.



(a)



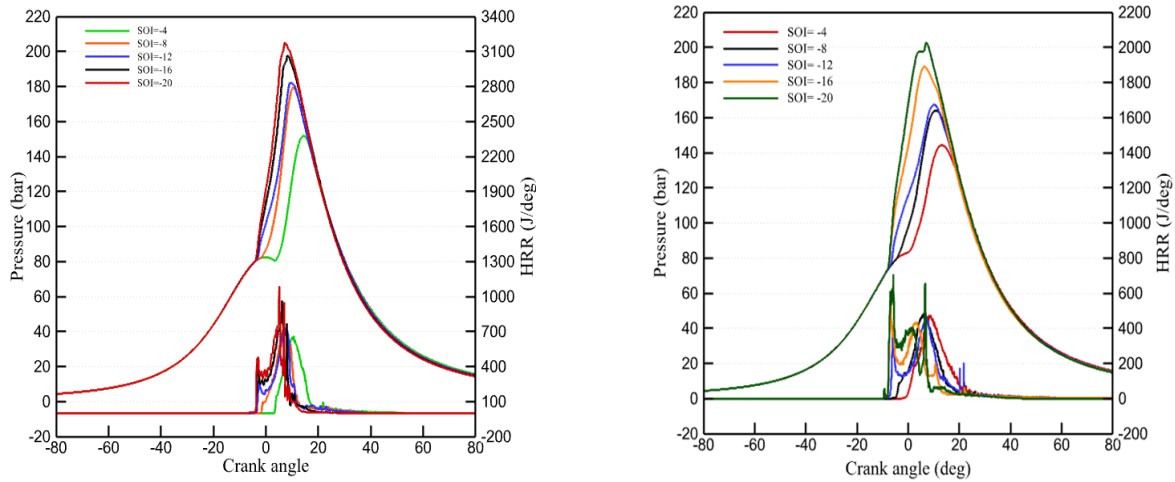
(b)



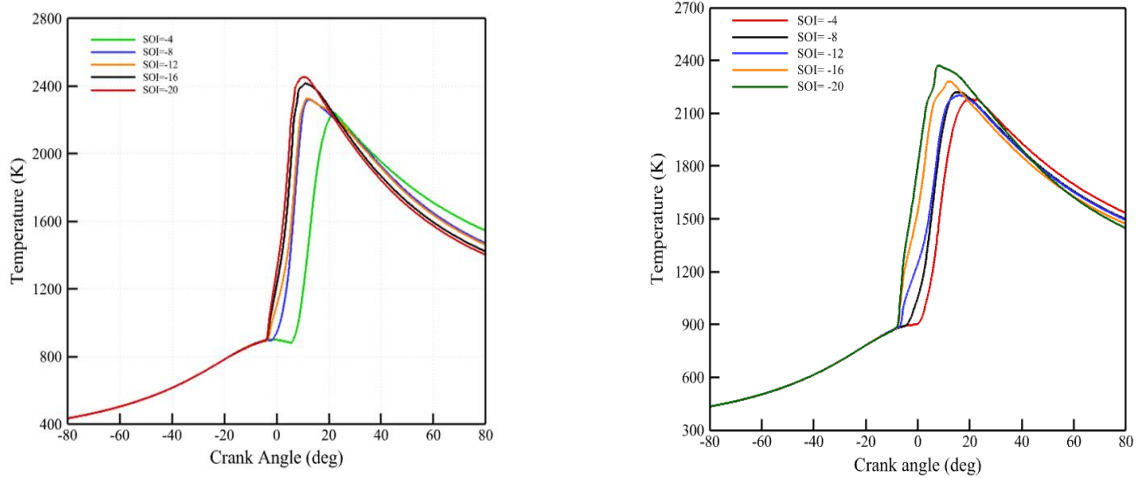
**Fig 8. volume with temperature lower than 2000 K at 7 CAD ATDC. a) Diesel/NG b) biodiesel/NG**

The crank angle at which a certain percentage of the heat is released, usually 10% and 90%, is a key factor in determining the start and end of combustion. Also, ignition delay (ID), which measures the time between direct fuel injection and ignition, plays a vital role in combustion analysis. In addition, CA50 which is mentioned as combustion phasing, describes the crank angle at which 50 % of the heat from combustion has been released. Combustion phasing affects the engine efficiency, power output, and emissions. Controlling the optimal combustion phasing can help achieve low temperature combustion, which reduces nitrogen oxide and particulate matter emissions.

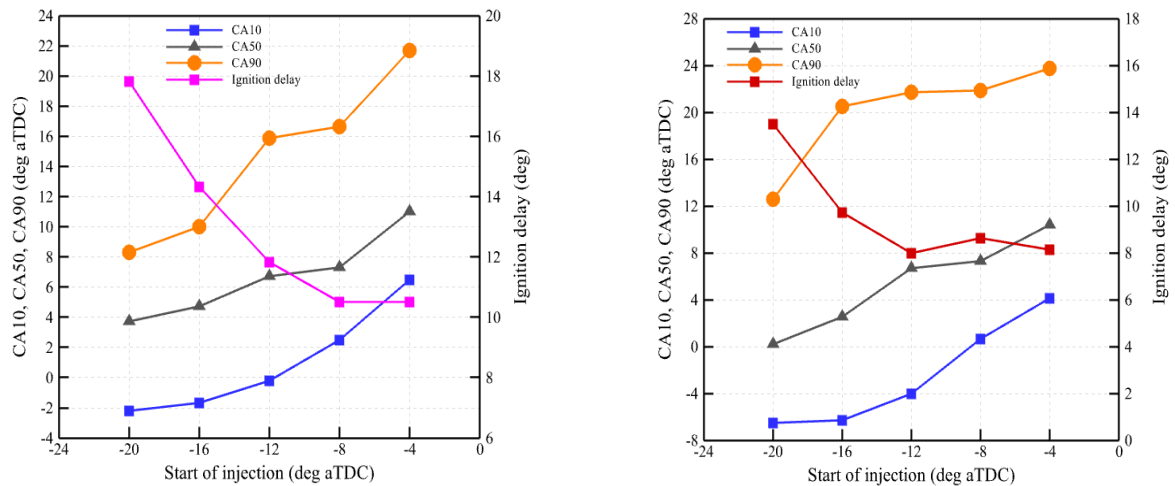
Figure 11 shows the CA10, CA50, CA90 and ignition delay for various injection timing of biodiesel/NG and diesel/NG.



(a) (b) **Fig. 9 In-cylinder pressure and heat rate release at different SOI a) biodiesel/NG b) diesel/NG**



(a) (b) **Fig. 10 In-cylinder temperature at different SOI a) biodiesel b) diesel**

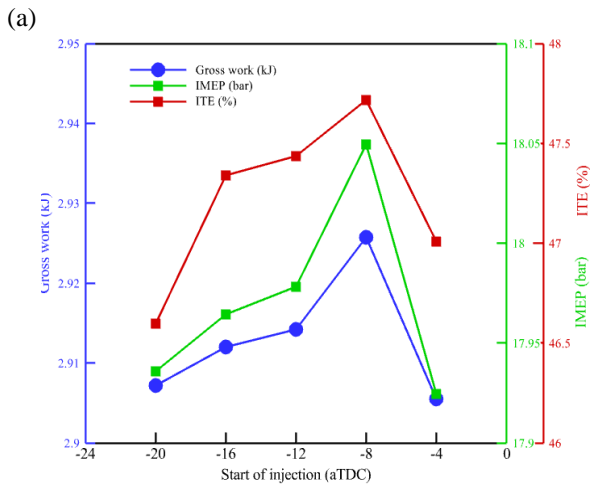
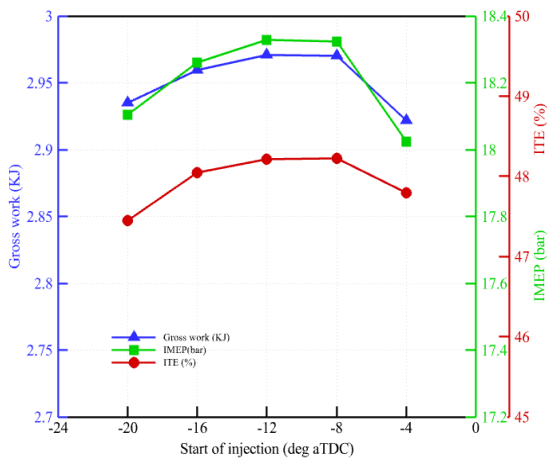


(a) (b) **Fig. 11 CA10, CA50, CA90, Ignition delay, burning duration at different start of injection a) biodiesel/NG b) diesel/NG**

At biodiesel/NG depending on the combustion chamber temperature and fuel concentration in the local area, ignition delay increases from 10.50 CAD for SOI= -4 CAD ATDC to 17.80 CAD for SOI= -20 CAD ATDC. Due to the fact that CA10 occurs prior to TDC within the range of SOI= -12 to SOI= -20, there is an increase in

Ignition delay. But in diesel/NG ignition delay increases from 8.13 CAD for SOI= -4 CAD ATDC to 13.51 CAD for SOI= -20 CAD ATDC. Ignition delay is influenced by several factors, such as the characteristics of the fuel and the operating condition of the engine while ignition delay





(a) **Fig 12. Gross work, IMEP, Indicated thermal efficiency at different injection timing a) biodiesel/NG b) diesel/NG**

affects the combustion efficiency, emissions, and noise of the engine.

Based on (Fig. 11 a), it can be observed that at SOI= -12, the CA10 value approximates the TDC but on (Fig. 11 b), in SOI= -8, the value of CA10 is near the TDC. Given that the temperature within the chamber at TDC is considerably elevated, this leads to improved combustion conditions.

According to (Fig. 11) the CA10-CA50, which exhibits an initial upward trend followed by a downward trend. This trend pattern indicates that combustion transpires in the vicinity of TDC at SOI= -12 for biodiesel/NG and SOI= -8 for diesel/NG, thereby facilitating diffusion and evaporation. Furthermore, the chart illustrates that the alterations in CA10-CA50 in comparison to CA50-CA90 are relatively minor, after which they escalate. This observation implies that the majority of combustion in the CA50-CA90 phase transpires in this region.

Figure (11) shows that CA50 occurs earlier when SOI is advanced for biodiesel/NG and diesel/NG. It was 11.01 degrees at SOI=-4, but it reduced to 3.7 degrees at SOI=-20 and for diesel/NG 10.41 degrees at SOI=-4, but it reduced to 0.23 degrees at SOI=-20.

At (Fig. 11 a) Combustion duration (difference between CA10 and CA90) decreases from 16 crank angle to 10 crank angle by advancing SOI from -4 to -20 CAD ATDC. Based on (Fig. 9) and (Fig. 10), advancing SOI led to higher in-cylinder pressure and temperature and as result, faster combustion and shorter combustion duration. But in diesel/NG, the trend is the opposite of biodiesel and it increases.

Figure 12 shows the gross work, indicated mean effective pressure and indicated thermal efficiency (ITE). As seen in this (Fig 12 a), IMEP increases at first when SOI is advanced and reaches its peak at SOI=-12, which is 18.33 bar. Then, IMEP decreases when SOI is further advanced and becomes 18.10 bar at SOI=-20. Gross work and ITE follow the same trend as IMEP, and they change similarly. But in (Fig 12 b), the trend is the same as (Fig 12 a), but the peak occurs in SOI= -8. Because in biodiesel/NG, CA10 is near in SOI=-12 around the TDC, but in diesel/NG in SOI=-8.

As shown in (Fig. 9), advancing SOI caused higher in-cylinder pressure and therefore, higher gross work. On the other hand, by more advancing SOI, based on (Fig. 11), start of combustion occurred very early and as result, negative work increased. Therefore, after SOI=-12 in biodiesel/NG and SOI= -8 in diesel/NG although in-cylinder pressure increased, but negative work also increased and IMEP decreased.

#### 4. CONCLUSION

In this study, the computational fluid dynamics tool which coupled with chemical kinetics mechanism are used to examine dual fuel combustion characteristics. It first compares the combustion features and emissions between diesel/NG and biodiesel/NG then it analyzes the biodiesel/NG combustion characteristics at different injection timing. The main findings are summarized as follows:

- In biodiesel/NG compared to diesel/NG, the mixture reactivity is higher because of the higher cetane number of biodiesel. This increases the maximum in-cylinder pressure by about 5%, and also increases the heat release rate by about 38%.
- Due to the occurrence of combustion in biodiesel/NG case at higher temperature than diesel/NG, and biodiesel combustion of characteristic the amounts of CO and UHC pollutants are reduced by 86% and 91%, respectively.
- Due to the occurrence of combustion in the case of biodiesel/NG at a higher temperature, with higher oxygen content, lower volatility and higher cetane number than diesel, the amount of CO and UHC pollutants is reduced by 86% and 91%, respectively.
- The combustion process in diesel/NG case starts in a confined central location, whereas in biodiesel/NG, it spreads over the cylinder and improves control of combustion which leads to lower CO emission.
- By advancing the SOI from -4 to -20 CAD ATDC, because of improving the mixing quality, the

maximum in-cylinder pressure increases from 150.2 bar to 205 bar. Also, the peak temperature in the cylinder increases and it is 2240 K at SOI=-4 while it is 2452 K at SOI=-20. But in diesel/NG the maximum in-cylinder pressure increases from 143.1 bar to 202.6 bar. Also, the peak temperature in the cylinder increases and it is 2180 K at SOI=-4 while it is 2370 K at SOI=-20.

- At biodiesel/NG gross work, IMEP and ITE increase by advancing the SOI from -4 to -12 CAD ATDC and after that they decrease. The maximum amount of IMEP, gross work and ITE are 18.3 bar, 2.97 kJ and 48.20%, respectively. But in diesel/NG at SOI=-8 aTDC the maximum amount of IMEP, gross work and ITE are 18.05 bar, 2.925 kJ and 47.70%.

## FUTURE WORK

In the future work, we will numerically investigate the effect of additives (hydrogen, oxygen, etc.) to biodiesel/natural gas in a dual fuel engine.

## CONFLICT OF INTEREST

The authors declare that they have no known competing financial interests or personal relationships that could have appeared to influence the work reported in this paper.

## AUTHORS CONTRIBUTION

**S. M. J. Yahyaei:** Investigation, Methodology, Software, Visualization, Validation, Formal analysis, Writing. **A. Gharehghani:** Project administration, Conceptualization, Supervision, Investigation, Review and editing. **M. Targohasemi:** Investigation, Methodology, Software, Visualization, Validation, Writing.

## REFERENCES

- Beale, J. C., & Reitz, R. (1999). Modeling Spray Atomization with the Kelvin-Helmholtz /Rayleigh-Taylor Hybrid Model. *Atomization Sprays*, 9, 623-650. <http://dx.doi.org/10.1615/AtomizSpr.v9.i6.40>.
- Bhave, N. A., Gupta, M. M., & Joshi, S. S. (2022). Effect of oxy hydrogen gas addition on combustion, performance, and emissions of premixed charge compression ignition engine. *Fuel Processing Technology*, 227(November 2021), 107098. <https://doi.org/10.1016/j.fuproc.2021.107098>.
- Cheng, X., Ng, H. K., Gan, S., Ho, J. H., & Pang, K. M. (2015). Development and validation of a generic reduced chemical kinetic mechanism for CFD spray combustion modelling of biodiesel fuels. *Combustion and Flame*, 162(6), 2354-2370. <https://doi.org/10.1016/j.combustflame.2015.02.003>
- Dal Forno Chuahy, F., Strickland, T., Walker, N. R., & Kokjohn, S. L. (2021). Effects of reformed fuel on dual-fuel combustion particulate morphology.

*International Journal of Engine Research*, 22(3), 777-790.

<https://doi.org/10.1177/1468087419879782>

- Duan, X., Lai, M. C., Jansons, M., Guo, G., & Liu, J. (2021). A review of controlling strategies of the ignition timing and combustion phase in homogeneous charge compression ignition (HCCI) engine. *Fuel*, 285(August 2020), 119142. <https://doi.org/10.1016/j.fuel.2020.119142>
- Fakhari, A. H., Gharehghani, A., Salahi, M. M., & Mahmoudzadeh Andwari, A. (2024). RCCI combustion of ammonia in dual fuel engine with early injection of diesel fuel. *Fuel*, 365, 131-182. <https://doi.org/10.1016/j.fuel.2024.131182>
- Fakhari, A. H., Gharehghani, A., Salahi, M. M., & Mahmoudzadeh Andwari, A., Mahmoudzadeh Andwari, A. et al. (2023). Numerical Investigation of Ammonia-Diesel Fuelled Engine Operated in RCCI Mode. *SAE Technical Paper*. <https://doi.org/10.4271/2023-24-0057>.
- Gharehghani, A., Abbasi, H. R., & Alizadeh, P. (2021). Application of machine learning tools for constrained multi-objective optimization of an HCCI engine. *Energy*, 233, 121106. <https://doi.org/10.1016/j.energy.2021.121106>
- Gharehghani, A., Hosseini, R., Mirsalim, M., & Jazayeri, S. A. (2015). An experimental study on reactivity controlled compression ignition engine fueled with biodiesel / natural gas. *Energy*, 1-10. <https://doi.org/10.1016/j.energy.2015.06.014>
- Harari, P. A., Banapurmath, N. R., Yaliwal, V. S., Khan, T. M. Y., Soudagar, M. E. M., & Sajjan, A. M. (2020). Experimental studies on performance and emission characteristics of reactivity controlled compression ignition (RCCI) engine operated with gasoline and Thevetia Peruviana biodiesel. *Renewable Energy*, 160, 865-875. <https://doi.org/10.1016/j.renene.2020.07.009>
- Hosseini, S. H., Tsolakis, A., Alagumalai, A., Mahian, O., Lam, S. S., Pan, J., Peng, W., Tabatabaei, M., & Aghbashlo, M. (2023). Use of hydrogen in dual-fuel diesel engines. *Progress in Energy and Combustion Science*, 98, 101100. <https://doi.org/10.1016/j.peccs.2023.101100>
- Huang, H., Zhu, Z., Chen, Y., Chen, Y., Lv, D., Zhu, J., & Ouyang, T. (2019). Experimental and numerical study of multiple injection effects on combustion and emission characteristics of natural gas-diesel dual-fuel engine. *Energy Conversion and Management*, 183, 84-96. <https://doi.org/10.1016/j.enconman.2018.12.110>
- Işik, M. Z., & Aydin, H. (2019). Investigation on the effects of gasoline reactivity controlled compression ignition application in a diesel generator in high loads using safflower biodiesel blends. *Renewable Energy*, 133, 177-189. <https://doi.org/10.1016/j.renene.2018.10.025>
- Jain, A., Jyoti Bora, B., Kumar, R., Sharma, P., Jyoti Medhi, B., Venkata Rambabu, G., & Deepanraj, B.

- (2023). Energy, exergy and emission [3E] analysis of Mesua Ferrea seed oil biodiesel fueled diesel engine at variable injection timings. *Fuel*, 353, 129115. <https://doi.org/10.1016/j.fuel.2023.129115>
- Kalsi, S. S., & Subramanian, K. A. (2017). Experimental investigations of effects of hydrogen blended CNG on performance, combustion and emissions characteristics of a biodiesel fueled reactivity controlled compression ignition engine (RCCI). *International Journal of Hydrogen Energy*, 42(7), 4548–4560. <https://doi.org/10.1016/j.ijhydene.2016.12.147>
- Karami, S., & Ghareghani, A. (2021). Effect of nano-particles concentrations on the energy and exergy efficiency improvement of indirect-injection diesel engine. *Energy Reports*, 7, 3273–3285. <https://doi.org/10.1016/j.egy.2021.05.050>
- Korkmaz, M., Ritter, D., Jochim, B., Beeckmann, J., Abel, D., & Pitsch, H. (2019). Effects of injection strategy on performance and emissions metrics in a diesel/methane dual-fuel single-cylinder compression ignition engine. *International Journal of Engine Research*, 20(10), 1059–1072. <https://doi.org/10.1177/1468087419836586>
- Kumar, M., Bhowmik, S., & Paul, A. (2022). Effect of pilot fuel injection pressure and injection timing on combustion, performance and emission of hydrogen-biodiesel dual fuel engine. *International Journal of Hydrogen Energy*, 47(68), 29554–29567. <https://doi.org/10.1016/j.ijhydene.2022.06.260>
- Lee, S., Kim, C., Lee, S., Lee, J., & Kim, J. (2020). Diesel injector nozzle optimization for high CNG substitution in a dual-fuel heavy-duty diesel engine. *Fuel*, 262, 116607. <https://doi.org/10.1016/j.fuel.2019.116607>
- Liu, J., Zhang, X., Liu, Y., Sun, P., Ji, Q., Wang, X., Li, Z., & Ma, H. (2023). Experimental study on in-cylinder combustion and exhaust emissions characteristics of natural gas/diesel dual-fuel engine with single injection and split injection strategies. *Process Safety and Environmental Protection*, 172, 225–240. <https://doi.org/10.1016/j.psep.2023.02.013>
- Mahla, S. K., Dhir, A., Gill, K. J. S., Cho, H. M., Lim, H. C., & Chauhan, B. S. (2018). Influence of EGR on the simultaneous reduction of NO<sub>x</sub>-smoke emissions trade-off under CNG-biodiesel dual fuel engine. *Energy*, 152(x), 303–312. <https://doi.org/10.1016/j.energy.2018.03.072>
- Mattarelli, E., Alberto Rinaldini, C., Caprioli, S., & Scignoli, F. (2022). Influence of H<sub>2</sub> enrichment for improving low load combustion stability of a Dual Fuel lightduty Diesel engine. *International Journal of Engine Research*, 23(5), 721–737. <https://doi.org/10.1177/14680874211051600>
- Mikulski, M., Balakrishnan, P. R., & Hunicz, J. (2019). Natural gas-diesel reactivity controlled compression ignition with negative valve overlap and in-cylinder fuel reforming. *Applied Energy*, 254, 113638. <https://doi.org/10.1016/j.apenergy.2019.113638>
- Mohan, B., Tay, K. L., Yang, W., & Chua, K. J. (2015). Development of a skeletal multi-component fuel reaction mechanism based on decoupling methodology. *Energy Conversion and Management*, 105, 1223–1238. <https://doi.org/10.1016/j.enconman.2015.08.060>
- Park, H., Shim, E., Lee, J., Oh, S., Kim, C., Lee, Y., & Kang, K. (2022). Large-squish piston geometry and early pilot injection for high efficiency and low methane emission in natural gas–diesel dual fuel engine at high-load operations. *Fuel*, 308, 122015. <https://doi.org/10.1016/j.fuel.2021.122015>
- Park, H., Shim, E., Lee, J., Oh, S., Kim, C., Lee, Y., & Kang, K. (2023). Comparative evaluation of conventional dual fuel, early pilot, and reactivity-controlled compression ignition modes in a natural gas-diesel dual-fuel engine. *Energy*, 268, 126769. <https://doi.org/10.1016/j.energy.2023.126769>
- Paykani, A., Chehrmonavari, H., Tsolakis, A., Alger, T., Northrop, W. F., & Reitz, R. D. (2022). Synthesis gas as a fuel for internal combustion engines in transportation. *Progress in Energy and Combustion Science*, 90, 100995. <https://doi.org/10.1016/j.pecs.2022.100995>
- Paykani, A., Garcia, A., Shahbakhti, M., Rahnama, P., & Reitz, R. D. (2021). Reactivity controlled compression ignition engine: Pathways towards commercial viability. *Applied Energy*, 282(PA), 116174. <https://doi.org/10.1016/j.apenergy.2020.116174>
- Pedrozo, V. B., Wang, X., Guan, W., & Zhao, H. (2022). The effects of natural gas composition on conventional dual-fuel and reactivity-controlled compression ignition combustion in a heavy-duty diesel engine. *International Journal of Engine Research*, 23(3), 397–415. <https://doi.org/10.1177/1468087420984044>
- Poorghasemi, K., Saray, R. K., Ansari, E., Irdmousa, B. K., Shahbakhti, M., & Naber, J. D. (2017). Effect of diesel injection strategies on natural gas/diesel RCCI combustion characteristics in a light duty diesel engine. *Applied Energy*, 199, 430–446. <https://doi.org/10.1016/j.apenergy.2017.05.011>
- Rajpoot, A. S., Choudhary, T., Chelladurai, H., Nath Verma, T., & Pugazhendhi, A. (2023). Sustainability analysis of spirulina biodiesel and their blends on a diesel engine with energy, exergy and emission (3E's) parameters. *Fuel*, 349, 128637. <https://doi.org/10.1016/j.fuel.2023.128637>
- Reitz, R. D., & Duraisamy, G. (2015a). Review of high efficiency and clean reactivity controlled compression ignition (RCCI) combustion in internal combustion engines. *Progress in Energy and Combustion Science*, 46, 12–71. <https://doi.org/10.1016/j.pecs.2014.05.003>
- Reitz, R. D., & Duraisamy, G. (2015b). Review of high efficiency and clean reactivity controlled compression ignition (RCCI) combustion in internal combustion engines. *Progress in Energy and*

- Combustion Science*, 46, 12–71.  
<https://doi.org/10.1016/j.pecs.2014.05.003>
- Sanjeevannavar, M. B., Banapurmath, N. R., Soudagar, M. E. M., Atgur, V., Hossain, N., Mujtaba, M. A., Khan, T. M. Y., Rao, B. N., Ismail, K. A., & Elfakhany, A. (2022). Performance indicators for the optimal BTE of biodiesels with additives through engine testing by the Taguchi approach. *Chemosphere*, 288(P2), 132450.  
<https://doi.org/10.1016/j.chemosphere.2021.132450>
- Schmidt, D. P., & Rutland, C. J. (2000). A New Droplet Collision Algorithm. *Journal of Computational Physics*, 164(1), 62–80.  
<https://doi.org/10.1006/jcph.2000.6568>
- Shu, J., Fu, J., Liu, J., Ma, Y., Wang, S., Deng, B., & Zeng, D. (2019). Effects of injector spray angle on combustion and emissions characteristics of a natural gas (NG)-diesel dual fuel engine based on CFD coupled with reduced chemical kinetic model. *Applied Energy*, 233–234, 182–195.  
<https://doi.org/10.1016/j.apenergy.2018.10.040>
- Shu, J., Fu, J., Liu, J., Zhang, L., & Zhao, Z. (2018). Experimental and computational study on the effects of injection timing on thermodynamics, combustion and emission characteristics of a natural gas (NG)-diesel dual fuel engine at low speed and low load. *Energy Conversion and Management*, 160, 426–438.  
<https://doi.org/10.1016/j.enconman.2018.01.047>
- Thangavel, V., Subramanian, B., & Ponnusamy, V. K. (2023). Investigations on the effect of H<sub>2</sub> and HHO gas induction on brake thermal efficiency of dual-fuel CI engine. *Fuel*, 337, 126888.  
<https://doi.org/10.1016/j.fuel.2022.126888>
- Thomas, J. J., Sabu, V. R., Nagarajan, G., Kumar, S., & Basrin, G. (2020). Influence of waste vegetable oil biodiesel and hexanol on a reactivity controlled compression ignition engine combustion and emissions. *Energy*, 206, 118199.  
<https://doi.org/10.1016/j.energy.2020.118199>
- Vargas-Ibáñez, L. T., Díaz-Ovalle, C. O., Cano-Gómez, J. J., & Flores-Escamilla, G. A. (2023). Theoretical analysis of the spray characteristics of ternary blends of diesel, biodiesel, and long-chain alcohols inside a combustion chamber. *Fuel*, 354.  
<https://doi.org/10.1016/j.fuel.2023.129305>
- Wei, L., & Geng, P. (2016). A review on natural gas / diesel dual fuel combustion, emissions and performance. *Fuel Processing Technology*, 142, 264–278.  
<https://doi.org/10.1016/j.fuproc.2015.09.018>
- Wei, Y., Zhang, Z., Li, X., Li, G., Zhou, M., & Belal, B. Y. (2023). The ignition characteristics of dual-fuel spray at different ambient methane concentrations under engine-like conditions. *Applied Thermal Engineering*, 219(PB), 119634.  
<https://doi.org/10.1016/j.applthermaleng.2022.119634>
- Wenming, Y., & Meng, Y. (2019). Phi-T map analysis on RCCI engine fueled by methanol and biodiesel. *Energy*, 187.  
<https://doi.org/10.1016/j.energy.2019.115958>
- Winangun, K., Setiyawan, A., & Sudarmanta, B. (2023). The combustion characteristics and performance of a Diesel Dual-Fuel (DDF) engine fueled by palm oil biodiesel and hydrogen gas. *Case Studies in Thermal Engineering*, 42.  
<https://doi.org/10.1016/j.csite.2023.102755>
- Wu, Z., Rutland, C. J., & Han, Z. (2019). Numerical evaluation of the effect of methane number on natural gas and diesel dual-fuel combustion. *International Journal of Engine Research*, 20(4), 405–423.  
<https://doi.org/10.1177/1468087418758114>
- Yin, X., Li, W., Duan, H., Duan, Q., Kou, H., Wang, Y., Yang, B., & Zeng, K. (2023). A comparative study on operating range and combustion characteristics of methanol/diesel dual direct injection engine with different methanol injection timings. *Fuel*, 334(P1), 126646.  
<https://doi.org/10.1016/j.fuel.2022.126646>
- Yousefi, A., Guo, H., & Birouk, M. (2019a). Effect of diesel injection timing on the combustion of natural gas/diesel dual-fuel engine at low-high load and low-high speed conditions. *Fuel*, 235, 838–846.  
<https://doi.org/10.1016/j.fuel.2018.08.064>
- Yousefi, A., Guo, H., & Birouk, M. (2020). Split diesel injection effect on knocking of natural gas/diesel dual-fuel engine at high load conditions. *Applied Energy*, 279, 115828.  
<https://doi.org/10.1016/j.apenergy.2020.115828>
- Yousefi, A., Guo, H., Birouk, M., & Liko, B. (2019b). On greenhouse gas emissions and thermal efficiency of natural gas/diesel dual-fuel engine at low load conditions: Coupled effect of injector rail pressure and split injection. *Applied Energy*, 242, 216–231.  
<https://doi.org/10.1016/j.apenergy.2019.03.093>
- Yu, H., Wang, W., Sheng, D., Li, H., & Duan, S. (2022). Performance of combustion process on marine low speed two-stroke dual fuel engine at different fuel conditions: Full diesel/diesel ignited natural gas. *Fuel*, 310.  
<https://doi.org/10.1016/j.fuel.2021.122370>
- Yuvenda, D., Sudarmanta, B., Wahjudi, A., & Hirowati, R. A. (2022). Effect of Adding Combustion Air on Emission in a Diesel Dual-Fuel Engine with Crude Palm Oil Biodiesel Compressed Natural Gas Fuels. *International Journal of Renewable Energy Development*, 11(3), 871–877.  
<https://doi.org/10.14710/ijred.2022.41275>
- Zarrinkolah, M. T., & Hosseini, V. (2022). Detailed Analysis of the Effects of Biodiesel Fraction Increase on the Combustion Stability and Characteristics of a Reactivity- Controlled Compression Ignition Diesel-Biodiesel/Natural Gas Engine. *Energies*, 15(3), 1–17.  
<https://doi.org/10.3390/en15031094>
- Zhang, Z., Lv, J., Li, W., Long, J., Wang, S., Tan, D., & Yin, Z. (2022). Performance and emission evaluation of a marine diesel engine fueled with natural gas ignited by biodiesel-diesel blended fuel. *Energy*, 256.  
<https://doi.org/10.1016/j.energy.2022.124662>